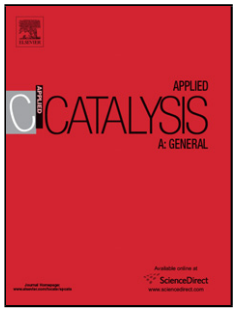

Title: Investigation of supported $Zn(OAc)_2$ catalyst and its stability in *N*-phenyl carbamate synthesis

Author: Fang Li Wenbo Li Jing Li Wei Xue Yanji Wang Xinqiang Zhao

PII: S0926-860X(14)00010-6
DOI: http://dx.doi.org/doi:10.1016/j.apcata.2014.01.008
Reference: APCATA 14646

To appear in: *Applied Catalysis A: General*

Received date: 18-8-2013
Revised date: 30-12-2013
Accepted date: 8-1-2014

Please cite this article as: F. Li, W. Li, J. Li, W. Xue, Y. Wang, X. Zhao, Investigation of supported $Zn(OAc)_2$ catalyst and its stability in *N*-phenyl carbamate synthesis, *Applied Catalysis A, General* (2014), http://dx.doi.org/10.1016/j.apcata.2014.01.008

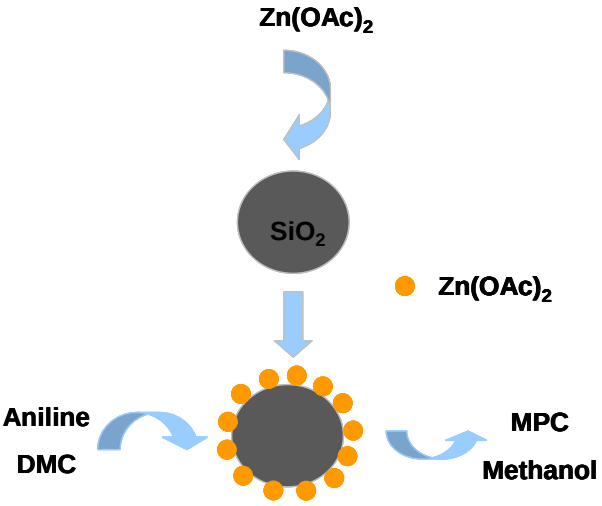

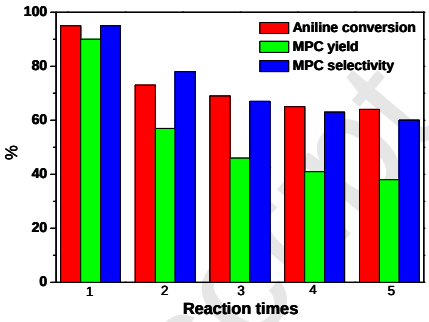

Stability of $Zn(OAc)_2/SiO_2$ catalyst

Highlights

·$Zn(OAc)_2/SiO_2$ was prepared by incipient impregnation.

·$Zn(OAc)_2/SiO_2$ shows the similar catalytic performance as $Zn(OAc)_2$.

·The stability of $Zn(OAc)_2/SiO_2$ improves considerably, but $Zn(OAc)_2$ can't be reused.

·The cause for the improved stability of $Zn(OAc)_2/SiO_2$ was investigated.

Investigation of supported $Zn(OAc)_2$ catalyst and its stability in *N*-phenyl carbamate synthesis

Fang Li[a]*, Wenbo Li[a], Jing Li[b], Wei Xue[a], Yanji Wang[a]*, Xinqiang Zhao[a]

[a] Hebei Provincial Key Lab of Green Chemical Technology & High Efficient Energy Saving, School of Chemical Engineering & Technology, Hebei University of Technology, Tianjin, 300130

[b] School of Civil Engineering, Hebei University of Technology, Tianjin, 300130

Abstract: $Zn(OAc)_2$ was found to give excellent catalytic performance for methyl *N*-phenyl carbamate (MPC) synthesis from aniline and dimethyl carbonate (DMC). However, after being used for only once it tended to lose activity because of the formation of ZnO by the reaction of $Zn(OAc)_2$ and methanol. $Zn(OAc)_2/SiO_2$ was prepared by incipient impregnation and it gave excellent catalytic performance in MPC synthesis, on which aniline conversion and MPC yield were 98.1% and 93.8%, respectively. And $Zn(OAc)_2/SiO_2$ was found to be more stable than $Zn(OAc)_2$ during the reaction. When $Zn(OAc)_2/SiO_2$ was used for the fifth time, aniline conversion and MPC yield were found to be 64.3% and 38.1%, respectively. The $Zn(OAc)_2/SiO_2$ catalyst was characterized by TG-DTA, ICP, FTIR, XRD and XPS. The characterization results suggested that the deactivation of $Zn(OAc)_2/SiO_2$ was also due to the formation of ZnO and there were two reasons for the improved stability of $Zn(OAc)_2/SiO_2$ catalyst. One was the formation of the Si–O–Zn bonds in $Zn(OAc)_2/SiO_2$ catalyst, which increased the steric hindrance of Zn and consequently retarded the reaction between $Zn(OAc)_2$ and methanol. The other cause was the dehydration between methanol and the hydroxyl group on the SiO_2 surface, which reduced the chance of a reaction between methanol and $Zn(OAc)_2$.

Keywords: *N*-phenyl carbamate, aniline, dimethyl carbonate, $Zn(OAc)_2/SiO_2$

*Corresponding author. Tel: +86 22 60203540; fax: +86 22 60204294.

E-mail address: lifang@hebut.edu.cn

1. Introduction

Methyl *N*-phenyl carbamate (MPC) is an intermediate for the preparation of methylene diphenyl diisocyanate (MDI), which is an important monomer for polyurethane synthesis. Initially, isocyanate was synthesized by the reaction between an amine and phosgene. This method results in environmental pollution and safety issues, and efforts are being made to develop non-phosgene routes such as the reductive carbonylation of nitrobenzene [1–4], the oxidative carbonylation of aniline [4–7] and the aminolysis of dimethyl carbonate (DMC). The reductive carbonylation of nitrobenzene and the oxidative carbonylation of aniline is carried out under higher temperatures and pressures, and a noble metal is used as the catalyst. However, the aminolysis of DMC for MDI synthesis is becoming more attractive. The reaction scheme for the synthesis of MDI from DMC is described in Scheme 1. In this process the only by-products are methanol and water. In addition, methanol is used as a raw material for the production of DMC by oxidative carbonylation, which will reduce the production cost of DMC.

In the first step of Scheme 1, a catalyst is required to achieve a better MPC yield. At present, the catalysts generally used in this reaction are zinc or lead compounds [8-15] as well as other oxide catalysts [16–20]. Among the catalysts, $Zn(OAc)_2$ often gives the best activity for aromatic carbamate synthesis. Gurgiolo [8] prepared MPC over a zinc acetate catalyst and the selectivity of MPC toward aniline was 99.8% at 140 °C and 0.88 MPa. Additionally, Baba [12] investigated the methoxycarbonylation of 2,4-toluene diamine and 4,4′-diphenylmethane diamine with DMC to their corresponding dicarbamates using $Zn(OAc)_2$ as a catalyst at 180 °C for 2 h. The yield of dimethyltoluene-2,4-dicarbamate was 96% while the yield of dimethyl-4,4′-methylenediphenyldicarbamate was 98%. Although $Zn(OAc)_2$ exhibits high conversion and selectivity, it possesses certain drawbacks. Apart from the separation and recovery of the generated homogeneous zinc acetate, it loses activity easily because of its transformation to ZnO by reaction with methanol and this is a byproduct in the reaction. To overcome these problems we prepared supported $Zn(OAc)_2$. Active carbon is the best support for these catalysts. Aniline conversion and MPC selectivity has been found to be 78.0% and 98.0%, respectively, for the $Zn(OAc)_2$/AC catalyst [13]. The catalytic activity of $Zn(OAc)_2$/AC is lower than that of $Zn(OAc)_2$. Furthermore, its stability was not investigated. In this paper we report the activity of

the $Zn(OAc)_2/SiO_2$ catalyst, which has almost the same catalytic activity as $Zn(OAc)_2$ but its stability was found to be better. The cause of $Zn(OAc)_2/SiO_2$ deactivation and the improvement in stability is also discussed in this paper.

2. Experimental

2.1 Catalyst preparation

The $Zn(OAc)_2/SiO_2$ catalyst was prepared by incipient impregnation. Appropriate amounts of $Zn(OAc)_2$ were dissolved in distilled water. The solution was impregnated into SiO_2. The impregnated samples were left overnight at room temperature and then dried under vacuum at 60 °C. Calcination was carried out at 300 °C for 2 h to obtain the $Zn(OAc)_2/SiO_2$ catalyst.

2.2 Catalytic evaluation

MPC was synthesized in a stainless steel autoclave. 1.0 ml aniline, 20 ml DMC and 0.28 g catalyst were added to the autoclave. The reaction temperature was 170 °C and the reaction time was 7 h. After the reaction, the reaction mixture was filtered to separate the catalyst and the filtrate was analyzed by high performance liquid chromatography (HPLC).

2.3 Product analysis

Waters HPLC was used to analyze the reaction liquid. The analytical conditions were as follows: A Kromasil C-18 (Φ4.6 mm×150 mm, 5 μm) chromatographic column was used at a flow rate of 0.4 ml/min. CH_3OH/H_2O (70/30, V/V) was used as the mobile phase and the detection wavelength was 254 nm. A quantitative analysis was carried out using nitrobenzene as the internal standard.

The product mixture was identified qualitatively using a Thermo Fisher TRACE DSQ GC-MS with a CP-SIL5CB (3.0 m×0.25 mm) capillary column. The injection port temperature was 250 °C. The column temperature was program-controlled and the initial column temperature was fixed at 40 °C for 3 min and then increased to 250 °C at a rate of 10 °C /min. The final temperature was maintained for 3 min. A mass spectrometer was used in Electron Impact (EI) mode at 200 °C.

2.4 Catalyst characterization

The Zn content of the catalyst was determined using a PerkinElmer Optima ICP 7300V.

X-ray diffraction patterns were recorded on a Rigaku D/MAX2500 with Cu K_α radiation at 40

kV and 100 mA. The scanning range was 3-80°.

Thermal analysis was performed using a Rigaku standard model TG-DTA analyzer. The sample was heated under air and the heating rate was 10 °C /min.

X-ray photoelectron spectroscopy was carried using a PHI-1600 ESCA SYSTEM. Mg K_α radiation at 300 W and 15 kV was used as the light source and the vacuum system was controlled at about 1.33×10^{-6} Pa. The binding energy values of the XPS signals were calibrated using adventitious C1s = 284.6 eV as a reference.

FTIR spectra were obtained with a NICOLET NEXUS-470 spectrometer. A DTGS detector was used and 32 scans were accumulated at a spectral resolution of 4 cm^{-1}.

Brunauer Emmett Teller (BET) surface area measurements were done using an ASAP 2020 instrument to analyze the specific surface area, the pore volume and the pore size distribution of the catalysts.

3. Results and discussion

3.1 Effect of $Zn(OAc)_2$ load on the catalytic performance of $Zn(OAc)_2/SiO_2$

The effect of $Zn(OAc)_2$ load on the catalytic performance of $Zn(OAc)_2/SiO_2$ is shown in Table 1 (entries 1–5). The aniline conversion and the MPC yield were found to be 37.2% and 5.2%, respectively, at a $Zn(OAc)_2$ load of 2%. Most of the aniline transformed into *N*-methylaniline (NMA) and *N*,*N*′-dimethylaniline (DMA). Aniline conversion increased with $Zn(OAc)_2$ load and a maximum of 98.4% was found for a $Zn(OAc)_2$ load of 20%. Upon increasing the $Zn(OAc)_2$ load continuously the aniline conversion decreased slightly. The cause might be that the pores of SiO_2 are thus blocked by $Zn(OAc)_2$ and ZnO for a small amount of $Zn(OAc)_2$ might be decomposed to ZnO. And the active surface area of the catalyst decreases with a higher $Zn(OAc)_2$ load. The catalyst activity decreases accordingly. Additionally, the MPC yield increased with $Zn(OAc)_2$ load and a maximum value of 93.8% was found for a $Zn(OAc)_2$ load of 30%. Therefore, 30 wt% was chosen as the $Zn(OAc)_2$ load.

The specific surface area and the pore structure of the $Zn(OAc)_2/SiO_2$ catalyst with different $Zn(OAc)_2$ loadings are summarized in Table 2. The specific surface area, pore volume and pore

size decrease with an increase in $Zn(OAc)_2$ loading. This is because $Zn(OAc)_2$and ZnO can block the pores of SiO_2. The X-ray diffraction patterns of the $Zn(OAc)_2/SiO_2$ catalysts with different loadings are shown in Fig. 1. There are no $Zn(OAc)_2$ diffraction peaks detected in the patterns. This phenomenon may be resulted by the small particle size of $Zn(OAc)_2$ which exceed the lower detection limit of the XRD apparatus. On the other hand, it may also be the result of the monolayer dispersion of $Zn(OAc)_2$ on SiO_2 surface. Xie et al [21] found that $Zn(OAc)_2$ could disperse on the surface of SiO_2 as a monolayer and the peaks of $Zn(OAc)_2$ crystalline would not appear in the XRD pattern if the contents of $Zn(OAc)_2$ on SiO_2 below the critical dispersion capacity.

3.2 Effect of calcination temperature on the catalytic performance of $Zn(OAc)_2/SiO_2$

To investigate the thermal decomposition of $Zn(OAc)_2$ supported on SiO_2, SiO_2, $Zn(OAc)_2$ and $Zn(OAc)_2/SiO_2$ (30 wt%, uncalcined) was characterized by TG-DTA and the profiles are shown in Fig. 2. In the TG-DTA profiles of SiO_2 (Fig.2A), there is an obvious weight loss between 50 ℃ and 180 ℃ and the weight loss is about 3.5%, which corresponds to the dehydration of the catalyst. There are two weight loss processes on the TG-DTA profiles of $Zn(OAc)_2$ (Fig.2B) accompanied by the absorption of heat. The first stage occurs between 50 ℃ and 100 ℃, which can be attributed to dehydration of $Zn(OAc)_2$. The second stage begins from about 220 ℃ to 340 ℃ and the weight loss is about 73%, which can be attributed to the decomposition of $Zn(OAc)_2$ for the decomposition temperature of $Zn(OAc)_2$ is about 240 ℃ [22]. Additionally on the DTA curve there is an exothermic peak approximately between 320 ℃ to 450 ℃. During the decomposition of $Zn(OAc)_2$ to ZnO, Timothy et al. [23] found that $Zn(OAc)_2$ was initially converted to acetic anhydride and ZnO, and then the acetic anhydride was converted into CO_2 and H_2O. Accordingly, the exothermic peak is attributed to the degradation of acetic anhydride. There is an endothermic peak between 50 ℃ and 200 ℃ on the DTA profile of $Zn(OAc)_2/SiO_2$ (Fig.2C) accompanied by obvious weight loss on the TG curve, which corresponds to the dehydration of the catalyst. From 200 ℃ to 500 ℃ two weight loss processes are evident on the TG curve. The first process occurs from 200 ℃ to 300 ℃ and the weight loss is only 3%. The first process is almost the same as that of $Zn(OAc)_2$. The second process occurs from 300 ℃ to 500 ℃ and the

weight loss is about 10%. Therefore, the thermal stability of most of the supported $Zn(OAc)_2$ is better than that of $Zn(OAc)_2$. This phenomenon indicates that the dispersion of $Zn(OAc)_2$ is not good on the SiO_2 surface. Some crystals might be in microcrystal form and their decomposition temperature is similar to that of $Zn(OAc)_2$, while some might have undergone monolayer dispersion and their decomposition temperature is higher than that of $Zn(OAc)_2$ for the interaction between $Zn(OAc)_2$ and SiO_2. Additionally on the DTA curve there is also an exothermic peak at approximately 400 °C to 500 °C, which is attributed to the degradation of acetic anhydride.

The effect of calcination temperature on the catalytic performance of $Zn(OAc)_2/SiO_2$ ($Zn(OAc)_2$ load was 30 wt%) is shown in Table 1 (entries 4,6–8). The $Zn(OAc)_2/SiO_2$ that was calcined at 300 °C exhibited better catalytic performance. At a calcination temperature of 400 °C the catalytic activity of $Zn(OAc)_2/SiO_2$ decreased slightly. However, as the calcination temperature increased steadily, the aniline conversion and the MPC yield decreased. The mole percent of byproduct, especially NMA and DMA, increased obviously. The cause is the decomposition of $Zn(OAc)_2$ to ZnO at higher temperatures and ZnO is known to have less catalytic activity toward MPC synthesis.

3.3 Catalytic performance and stability comparison between $Zn(OAc)_2/SiO_2$ and $Zn(OAc)_2$

Table 3 shows the catalytic performance of $Zn(OAc)_2/SiO_2$ and $Zn(OAc)_2$ with the same amount of Zn. As for $Zn(OAc)_2$, aniline conversion nearly reached 100% at different reaction time. However, MPC yield increased and a maximum of 96.5% was found for a reaction time of 5 h. Upon prolonging the reaction time continuously MPC yield changed slightly. As for $Zn(OAc)_2/SiO_2$, the aniline conversion and MPC yield increased with reaction time. The maximal value was obtained with a reaction time of 7h, giving an aniline conversion of 98.1% and a MPC yield of 93.8%. In addition, the turnover number (TON) over $Zn(OAc)_2$ was almost the same at different time. Compared with $Zn(OAc)_2$, the TON over $Zn(OAc)_2/SiO_2$ increased with reaction time. When the reaction time was less than 5h, the TON over $Zn(OAc)_2/SiO_2$ was

lower than that of $Zn(OAc)_2$. Once the reaction time prolonged to 7 h, they were almost the same.

The stability of $Zn(OAc)_2/SiO_2$ was also investigated. After the reaction, the used $Zn(OAc)_2/SiO_2$ catalyst was washed with DMC and dried, and was then reused in a following reaction under the same conditions. The results are shown in Fig. 3. Aniline conversion and MPC selectivity decrease obviously after second use as the aniline conversion and MPC yield were found to be 73.2% and 57.5%, respectively. However, with further reuse, the aniline conversion and MPC selectivity decreased but smoothly. After using $Zn(OAc)_2/SiO_2$ 5 times, the aniline conversion and MPC yield were found to be 64.3% and 38.1%, respectively.

The stability of $Zn(OAc)_2$ was also investigated for comparison. After $Zn(OAc)_2$ was used once it showed almost no further activity toward MPC synthesis because aniline conversion and MPC yield were found to be 9.2% and 1.7%, respectively. Therefore, $Zn(OAc)_2$ is prone to a loss of activity and cannot be reused.

The deactivated $Zn(OAc)_2$ was characterized by XRD and the result is shown in Fig. 4(b). $Zn(OAc)_2$ disappears completely and ZnO is formed after single use. ZnO has almost no activity toward MPC synthesis. We also found that $Zn(OAc)_2$ pretreated with methanol at 170 °C for 3 h was completely transformed into ZnO. Therefore, the cause of $Zn(OAc)_2$ deactivation is the formation of ZnO by the reaction between $Zn(OAc)_2$ and methanol. The reaction equation of $Zn(OAc)_2$ and methanol is as follows [24]:

$$Zn(OCOCH_3)_2 + 2\,CH_3OH \longrightarrow 2\,CH_3COOCH_3 + ZnO + H_2O$$

Similarly, $Zn(OAc)_2/SiO_2$ was pretreated with methanol at 170 °C for 7 h and then the pretreated $Zn(OAc)_2/SiO_2$ was used in the reaction between aniline and DMC. We found that the catalytic activity of pretreated $Zn(OAc)_2/SiO_2$ decreased because the aniline conversion decreased to 67.9% and the MPC yield decreased to 57.0%, which is close to that of the $Zn(OAc)_2/SiO_2$ that was used a second time. The solution obtained after pretreatment with methanol was analyzed by GC-MS. The results show that a small amount of methyl acetate is present in the solution, which indicates that some of the $Zn(OAc)_2$ on the SiO_2 surface reacted with methanol to form ZnO.

To understand the cause of $Zn(OAc)_2/SiO_2$ deactivation, $Zn(OAc)_2/SiO_2$, $Zn(OAc)_2/SiO_2$

pretreated with methanol ($Zn(OAc)_2/SiO_2$-ME) and deactivated $Zn(OAc)_2/SiO_2$ ($Zn(OAc)_2/SiO_2$-DE) were characterized. The XRD patterns of these catalysts are shown in Fig. 4. No diffraction peak was present for these catalysts (Fig. 4c, Fig. 4d, Fig. 4e).

FTIR spectra of these catalysts are shown in Fig. 5. The FTIR spectrum of $Zn(OAc)_2$ (Fig. 5a) has bands at 1557 cm^{-1} and 1448 cm^{-1} that are attributed to the asymmetric and symmetric stretching vibration of COO^- in $Zn(OAc)_2$. For the SiO_2 spectrum (Fig. 5b), the Si–O–Si asymmetric and symmetric stretching vibration bands are at 1104 cm^{-1} and 471 cm^{-1}. The bands at 804 cm^{-1} and 971 cm^{-1} are attributed to the asymmetric and symmetric stretching vibrations of O–Si–O [25]. Compared with SiO_2 the spectra of $Zn(OAc)_2/SiO_2$ (Fig. 5c), $Zn(OAc)_2/SiO_2$-ME (Fig. 5d) and $Zn(OAc)_2/SiO_2$-DE (Fig. 5e) show that the band at 971 cm^{-1} broadens toward the low-frequency side and simultaneously the band at 477 cm^{-1} broadens toward the high-frequency side, which is caused by the presence of the Si–O–Zn bonds. The Si–O–Zn vibration bands are at about 940 cm^{-1} and 546 cm^{-1} [26]. The interaction between $Zn(OAc)_2$ and SiO_2 results in the formation of the Si–O–Zn bonds. For $Zn(OAc)_2/SiO_2$ (Fig. 5c), the asymmetric stretching vibration band for COO^- shifts to a higher frequency and that of the COO^- symmetric stretching vibration broadens toward the low-frequency region. This might come from the interaction between $Zn(OAc)_2$ and SiO_2. The coordination mode of Zn and O in $Zn(OAc)_2$ can be illustrated as follows where anhydrous zinc acetate adopts a polymeric structure consisting of zinc coordinated to four oxygen atoms in a tetrahedral environment with each tetrahedron being connected to neighbors by acetate groups [27].

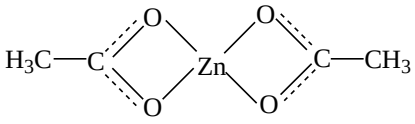

Once $Zn(OAc)_2$ is loaded onto the surface of SiO_2, the coordination mode of the Zn and acetate groups changes from bidentate coordination to single dentate coordination (illustrated as A and B), and this comes from the formation of the Si–O–Zn bonds, which release some O atoms in the acetate groups from the coordination. Accordingly, the COO^- stretching vibration band broadens toward the low-frequency side.

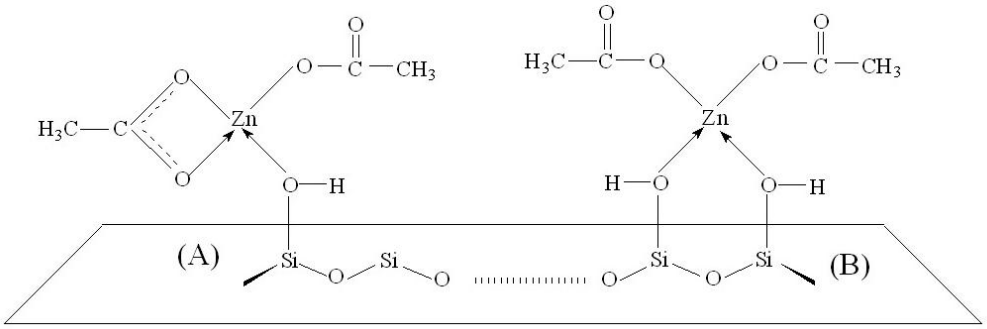

Additionally, the band intensity of the COO^- stretching vibration decreased obviously for $Zn(OAc)_2/SiO_2$-ME (Fig. 5d) and $Zn(OAc)_2/SiO_2$-DE (Fig. 5e), which reveals a decrease in the $Zn(OAc)_2$ content on the surface of the SiO_2. There are two causes for this decrease: one is the formation of ZnO by the reaction between $Zn(OAc)_2$ and methanol and the other is the leakage of $Zn(OAc)_2$. Therefore, the Zn contents of $Zn(OAc)_2/SiO_2$, $Zn(OAc)_2/SiO_2$-ME and $Zn(OAc)_2/SiO_2$-DE were analyzed by ICP and the results are 14.2%, 13.4% and 14.6%, respectively. There is, therefore, no obvious leakage of Zn in $Zn(OAc)_2/SiO_2$-DE and $Zn(OAc)_2/SiO_2$-ME. The cause of $Zn(OAc)_2/SiO_2$ deactivation is thus the formation of ZnO.

3.4 Reason for the stability of $Zn(OAc)_2/SiO_2$

From the aforementioned results, both $Zn(OAc)_2$ and $Zn(OAc)_2/SiO_2$ exhibit good catalytic performance for MPC synthesis. However, $Zn(OAc)_2$ is prone to a loss in activity because of its reaction with methanol to form ZnO. Once $Zn(OAc)_2$ is supported on SiO_2 the stability of $Zn(OAc)_2/SiO_2$ improves considerably.

To determine the reason for the stability of $Zn(OAc)_2/SiO_2$ the interaction between $Zn(OAc)_2$ and SiO_2 needs to be understood. $Zn(OAc)_2$, SiO_2 and $Zn(OAc)_2/SiO_2$ were characterized by XPS and the results are shown in Table 4. Compared with $Zn(OAc)_2$ and SiO_2, the binding energy of Si 2*p* and O 1*s* in $Zn(OAc)_2/SiO_2$ is different. This might be due to the replacement of the Si–O–Si bonds by Si–O–Zn bonds while $Zn(OAc)_2$ is supported on the SiO_2 surface. In addition, the binding energy of the Zn 2*p*3 in $Zn(OAc)_2/SiO_2$ does not change by comparison with $Zn(OAc)_2$. Besides The Si–O–Zn bond, the CO–O–Zn bond are also present in the $Zn(OAc)_2/SiO_2$ catalyst. Therefore, it is assumed that the formation of a Si–O–Zn bond has little effect on the binding

energy of Zn 2*p*3.

Many researchers have investigated the reaction between $Zn(OAc)_2$ and methanol to form ZnO and found that the important intermediate product $Zn_5(OH)_8(Ac)_2{\cdot}2H_2O$ is formed initially. This is referred to as layered hydroxide zinc acetate (LHZA), which then undergoes hydrolysis and inorganic polymerization leading to the formation of ZnO [28–30]. When $Zn(OAc)_2$ is supported on SiO_2, the Si–O–Zn bonds are formed by the interaction between SiO_2 and $Zn(OAc)_2$. Compared with free Zn^{2+} the formation Si–O–Zn bonds imposes steric hindrance on the Zn present on SiO_2, which retards the formation of $Zn_5(OH)_8(Ac)_2{\cdot}2H_2O$ and thus the formation of ZnO.

Additionally, an interaction exists between methanol and SiO_2. SiO_2 was pretreated with methanol at 170 °C for 7 h and characterized by FTIR, and the result is shown in Fig. 5f Compared with SiO_2 (Fig. 5b), three new bands appear in the spectrum of SiO_2 pretreated with methanol. The bands at 2960 cm^{-1} and 2860 cm^{-1} are attributed to the stretching vibration of C–H in methyl groups while the band at 1465 cm^{-1} is attributed to the bending vibration of C–H in methyl groups. Therefore, methyl groups are present on the SiO_2 surface after SiO_2 was pretreated with methanol. This is due to the dehydration reaction between methanol and the hydroxyl group on the SiO_2 surface and the reaction is as follows [31]:

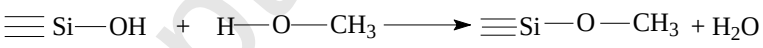

From the above analysis, we believe that there are two causes for the stability of the $Zn(OAc)_2/SiO_2$ catalyst. One is the formation of the Si–O–Zn bonds in the $Zn(OAc)_2/SiO_2$ catalyst, which increases the steric hindrance of Zn and consequently retards the reaction between $Zn(OAc)_2$ and methanol. The other cause is the dehydration of methanol and hydroxyl groups on the SiO_2 surface, which reduces the chance of a reaction between methanol and $Zn(OAc)_2$.

Additionally, Fig. 3 shows that upon $Zn(OAc)_2/SiO_2$ catalyst reuse, aniline conversion and MPC selectivity decreases obviously. However, with further reuse the aniline conversion and MPC selectivity decreases but smoothly. The cause might be the poor dispersion of $Zn(OAc)_2$ on the surface of SiO_2. Some monolayer dispersion may occur but this is not complete, which might result in some $Zn(OAc)_2$ not interacting with SiO_2 to form the Si–O–Zn bonds and a reaction with

methanol may easily result in the formation of ZnO. Therefore, the catalytic performance of $Zn(OAc)_2/SiO_2$ decreases obviously upon reuse. Once this part of $Zn(OAc)_2$ is entirely transformed to ZnO, the catalytic performance of $Zn(OAc)_2/SiO_2$ decreases steadily.

Thus it can be seen that the formation of Si–O–Zn bond plays an important role in the stability of $Zn(OAc)_2/SiO_2$. And to increase the stability of the catalyst, more Si–O–Zn bonds should be created, which can be achieved by the improved dispersion of $Zn(OAc)_2$ on SiO_2 surface. Xie et al [21] found that spontaneous monolayer dispersion of oxides and salts on supports was a wide-spread phenomenon. When the content of oxides and salts on supports exceeded the critical dispersion capacity, there would be a crystalline phase of oxides and salts. The critical dispersion capacity or the threshold value was almost linearly proportional to the specific surface area of the support. They also found that $Zn(OAc)_2$ could disperse spontaneously on the surface of SiO_2 as a monolayer at a temperature close to their melting points. So it can be speculated that more Si–O–Zn bonds can be created using SiO_2 with large specific surface area as support and the stability of $Zn(OAc)_2/SiO_2$ catalyst can be improved accordingly.

3.5 A possible reaction mechanism for aniline and DMC over $Zn(OAc)_2/SiO_2$ catalyst

The reaction mechanism for the carbamate synthesis by the reaction of amine and DMC over homogenously Lewis acid catalyst has been investigated widely [33–38]. It is generally believed that the carbonyl of DMC can interact with nucleophiles for its polarized positive charge and sp^2 hybridization of C atom [33, 34]. Over Lewis acid catalyst, there are two different opinions on the catalytic mechanism. Some people reported that the carbonyl group of DMC could be activated by the catalyst, which could facilitate the nucleophilic attack accordingly [11,35-37]. And others thought that the amino group could be activated by the catalyst [38]. Similarly, using $Zn(OAc)_2$ as catalyst, Baba et al [11] have proposed that the carbonyl of DMC coordinates to Zn^{2+} to form an intermediate (Species A). They also reported that methanol which is the by product could help to transform the bidentate coordination of $CH_3COO_2^{-1}$ to Zn^{2+} into monodentate coordination and then facilitated the coordination of DMC to Zn^{2+}. On the contrary, Xiao et al [38] have suggested that the amino group only can interact with $Zn(OAc)_2$ to form the zinc complex (Species B), which further react with DMC to produce carbamate.

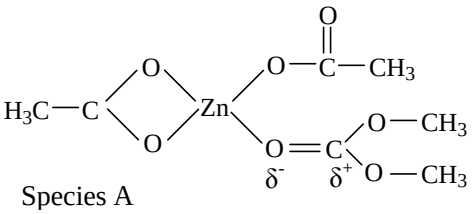

Species A

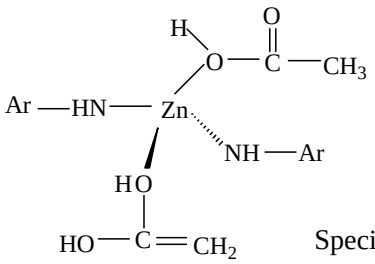

Species B

As aforementioned in 3.3, there are two modes for the coordination of Zn^{2+} with acetate group in $Zn(OAc)_2/SiO_2$. With reguard to mode A, the O atom of the carbonyl group in DMC or the N atom of the amino group in aniline may have the chance to coordinate with Zn^{2+}. However, unlike $Zn(OAc)_2$, $Zn(OAc)_2/SiO_2$ is a heterogeneous catalyst and there exits the resistance for the reactants to diffuse to the catalyst surface, which can be seen from the results showed in Table 3 that the TON of $Zn(OAc)_2/SiO_2$ is lower than that of $Zn(OAc)_2$ in the initial stage of the reaction and they are almost the same in latter stage. Furthermore, DMC is largely excessive during the reaction. So it is presumed that more chances for DMC to coordinate with Zn^{2+} and the reaction mechanism is illustrated in scheme 2.

As for the mode B, Zn cannot coordinate with O atom or N atom for it has reached the stable construction of 18 electrons. Thus the mode B does not have the catalytic activity for MPC synthesis. However, $Zn(OAc)_2/SiO_2$ exhibits excellent catalytic performance for MPC synthesis. Thus the coordination mode of B is few in $Zn(OAc)_2/SiO_2$ catalyst.

4. Conclusion

At a $Zn(OAc)_2$ loading of 30 wt% and calcination temperature of 300 °C, $Zn(OAc)_2/SiO_2$ shows excellent catalytic activity toward MPC synthesis with an aniline conversion of 98.1% and a MPC yield of 93.8%. Moreover, it is more stable than $Zn(OAc)_2$. After 5 cycles of $Zn(OAc)_2/SiO_2$ use, aniline conversion and MPC yield was found to be 64.3% and 38.1%, respectively. The reason for $Zn(OAc)_2/SiO_2$ deactivation is the formation of ZnO by a reaction between methanol and $Zn(OAc)_2$. For the $Zn(OAc)_2/SiO_2$ catalyst, the thermal stability of most supported $Zn(OAc)_2$ improves obviously compared with that of $Zn(OAc)_2$, and this is due to the interaction between $Zn(OAc)_2$ and SiO_2 leading to the formation of a Si–O–Zn bond. In addition, the presence of a Si–O–Zn bond in the $Zn(OAc)_2/SiO_2$ catalyst has an important effect on the improvement of $Zn(OAc)_2/SiO_2$ stability as the steric hindrance of Zn increases and, consequently, the reaction

between $Zn(OAc)_2$ and methanol is retarded. Another reason for the improvement in $Zn(OAc)_2/SiO_2$ stability is the dehydration between methanol and the hydroxyl groups on the SiO_2 surface, which reduces the possibility of a reaction between methanol and $Zn(OAc)_2$.

Acknowledgements

This work was supported by the National Natural Science Foundation of China (No. 21106031, 21176056) and the Natural Science Foundation of Hebei (No. B2011202139).

References

[1]A. Krogul, J. Skupińska, G. Litwinienko, J. Mol. Catal. A: Chem. 337(2001)9-16

[2]F. Shi, Y. He, D. Li, Y. Ma, Q. Zhang, Y. Deng, J. Mol. Catal. A: Chem. 244(2006)64-67

[3]F. Ragaini, S. Cenini, J. Mol. Catal. A: Chem. 161(2000)31-38

[4]F. Ragaini, Dalton Trans. 32(2009)6251-6266

[5]M. Honda, S. Sonehara, H. Yasuda, Y. Nakagawa, K. Tomishige, Green Chem.13(2011) 3406-3413

[6]B. Chen, S. S. C. Chuang, J. Mol. Catal. A: Chem. 195(2003)37-45.

[7]H. S. Kim, Y. J. Kim, H. Lee, S. D. Lee, C. S. Chin, J. Catal.184(1999)526-534.

[8]A. E. Gurgiolo, U.S. Patent 4,268,683(1981).

[9]Y. Wang, X. Zhao, F. Li, S. Wang, J. Zhang，J. Chem. Technol. Biotechnol. 76(2001)857-861.

[10]W. Xue, J. Cong, F. Li, X. Zhao, Y. Wang, Acta Petrol. Sin. 18(2002)50-55.

[11]T. Baba,A. Kobayashi,Y. Kawanam, K. Inazu, A. Ishikawa, T. Echizenn, K. Murai, S. Asoc, M. Inomata, Green Chem. 7(2005)159-165.

[12]T. Baba, A. Kobayashi, H. Tanaka, H. Tanaka, S. Aso,M. Inomata, Y. Kawanami, Catal. Lett. 82(2002) 193-197.

[13]X. Zhao, Y. Wang, S. Wang, H. Yang, J. Zhang, Ind. Eng. Chem. Res. 41(2002)5139-5144.

[14]Z. Fu, Y. Ono, J. Mol. Catal. A: Chem. 91(1994)399-405.

[15]T. Baba, M. Fujiwara, A. Oosaku, A. Kobayashi, R. G. Deleon, Y. Ono, Appl. Catal. A:Gen.

227(2002)1-6.

[16]N. Katada, H. Fujinaga, Y. Nakamura, K. Okumura, K. Nishigaki, M. Niwa, Catal. Lett. 80(2002)47-51.

[17]W. Kang, T. Kang, F. Ma, Y. Zhao, L.Cui, J. Yao, G. Wang, Chin. J. Catal. 28(2007)5-9.

[18]Q. Li, J. Wang, W. Dong, M. Kang, X. Wang, S. Peng, Chin. J. Catal. 24(2003) 639-642.

[19]F. Li, J. Miao, Y. Wang, X. Zhao, Ind. Eng. Chem. Res. 45(2006)4892-4897.

[20]F. Li, Y. Wang, W. Xue, X. Zhao, J. Chem. Technol. Biotechnol. 84(2009) 48-53.

[21] Y. Xie , Y. Tang, Advan. Catal. 37(1990)1-43

[22]M. Ohyama, H. Kozuka, T.Yoko, Thin Solid Films. 306 (1997) 78-85

[23]T. Biswick, W. Jones, A. Pacula, E. Serwicka, J. Podobinski, Solid State Sci. 11(2009)330-335.

[24]P. Tonto, O. Mekasuwandumrong, S. Phatanasri, V. Pavarajarn, P. Praserthdama, Ceram. Int. 34(2008)57-62

[25]P. A. Tanner, B. Yan, H. Zhang, J. Mater. Sci. 35(2000)4325-4328

[26]A. Roy, S. Polarz, S. Rabe, B. Rellinghaus, H. Zähres, F. E. Kruis, M. Driess, Chem.-A Eur. J. 10(2004)1565-1575

[27]W. Clegg, I. R. Little, B. P. Straughan, Acta. Cryst. C42 (1986) 1701-1703

[28]E. Hosono, S. Fujihara, T. Kimura, H. Imai, J. Colloid Interface Sci. 272(2004)391-393

[29]L. Znaidi, Mater. Sci. Eng. B. 174(2010)18-30

[30]E. Hosono, S. Fujihara, T. Kimura, H. Imai, J. Sol-gel Sci. Technol.29(2004)71-79

[31]T. R. Forester, R. F. Howe, J. Am. Chem. Soc. 109(1987)5076-5082

[32] Y. Xie, Y. Tang, Advan. Catal. 37(1990) 1-43

[33]P. Tundo, L. Rossi, A. Loris, J. Org. Chem. 70(2005)2219-2224

[34]P.Tundo, S. Bressanello, A. Loris, G. Sathicq, Pure Appl. Chem. 77(2005)1719-1725

[35]M. Distaso, E. Quaranta, Appl. Catal. B: Environ. 66 (2006) 72-80

[36]X. Fu, Z. Zhang, C. Li, L. Wang, H. Ji, Y. Yang, T. Zou, G. Gao, Catal. Commun. 10 (2009) 665-668

[37]L. Zhang, Y. Yang, Y. Xue, X. Fu, Y. An, G. Gao, Catal. Today. 158 (2010) 279-285

[38]F. Xiao, D. Zhang, Q. Dong, W. Wei,Y. Sun, React.Kinet.Catal.Lett. 89(2006)131-138

Figure1

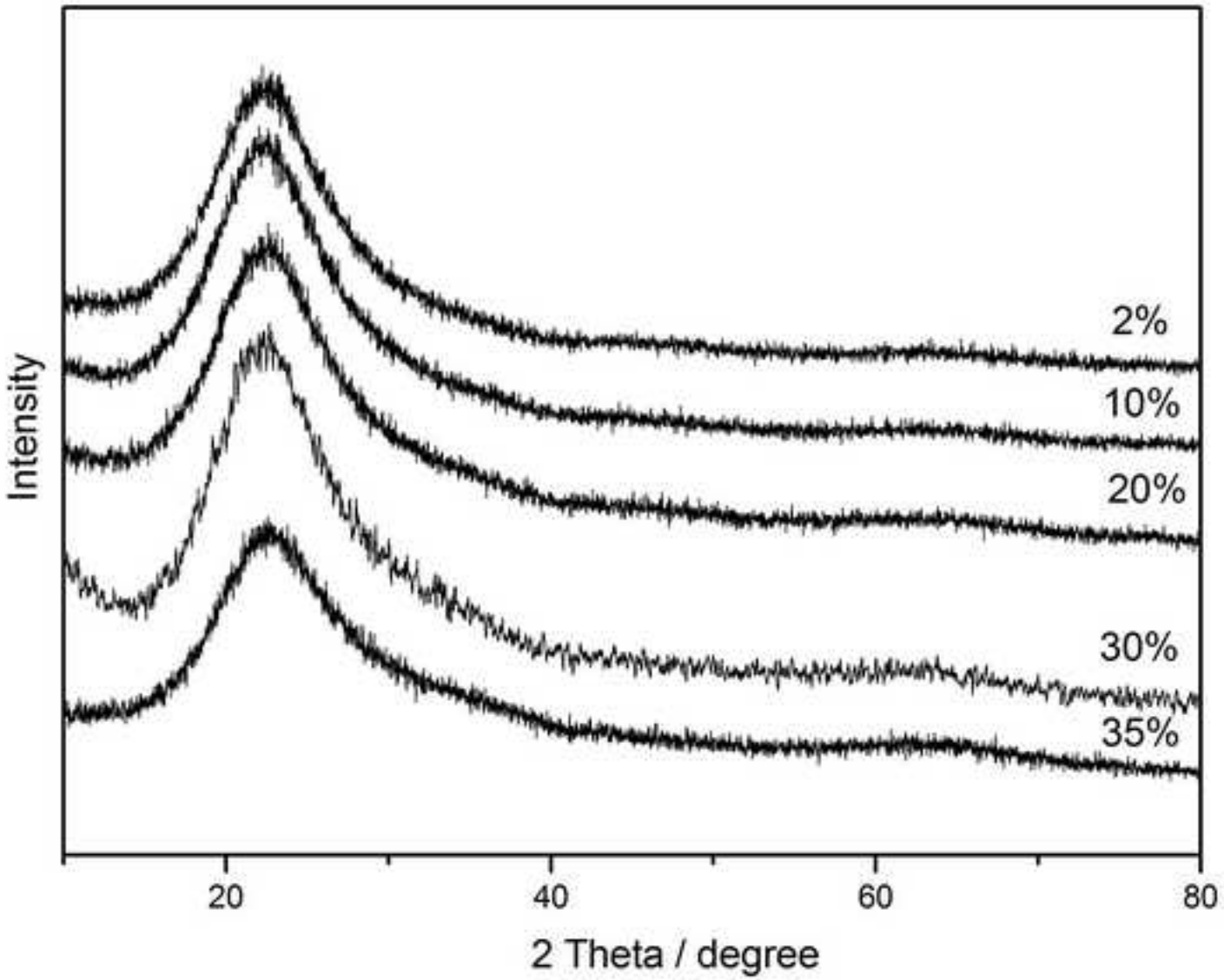

Figure2A

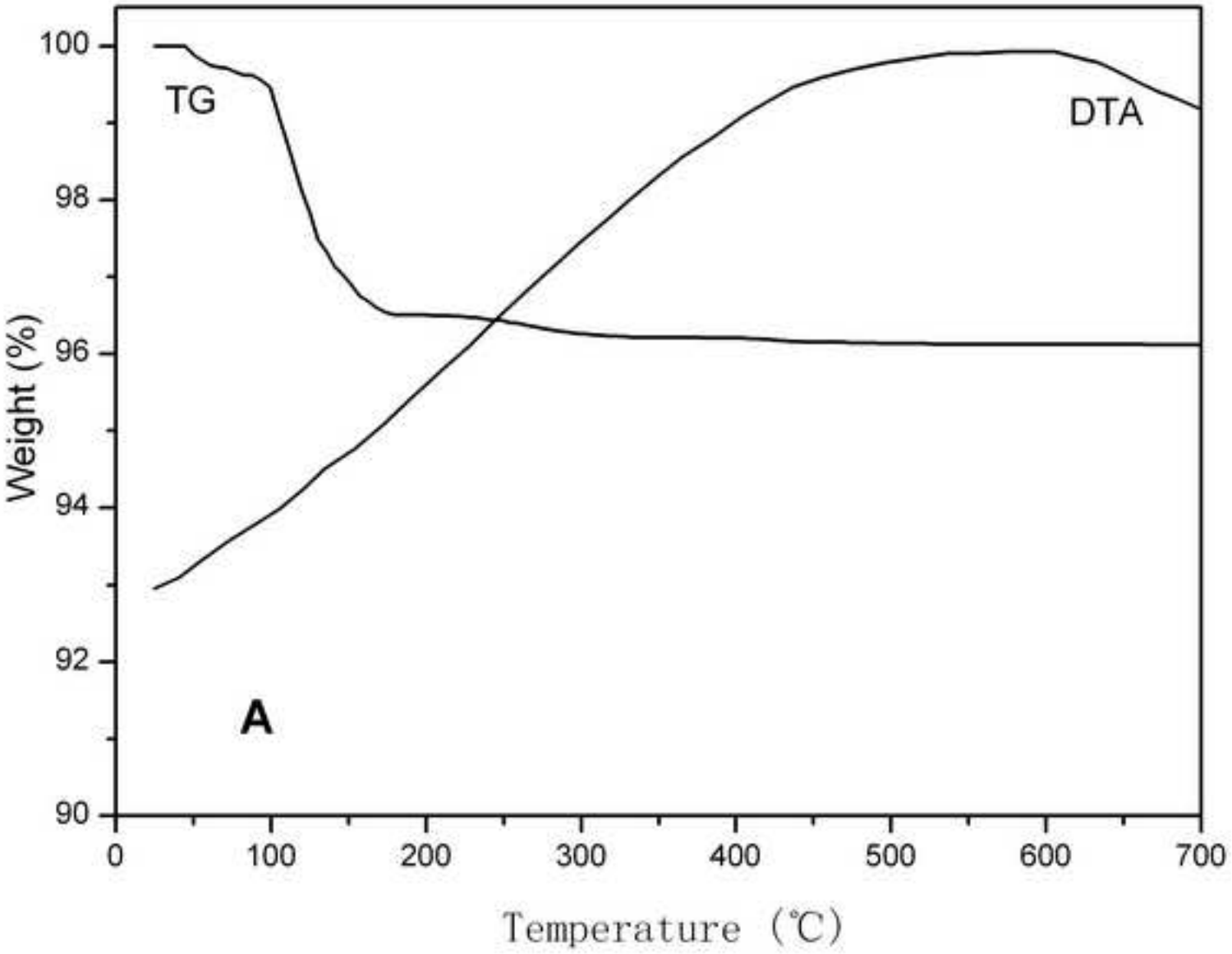
100
98
96
94
92
90
Weight (%)
TG
DTA
A
0
100
200
300
400
500
600
700
Temperature (℃)

Figure2B

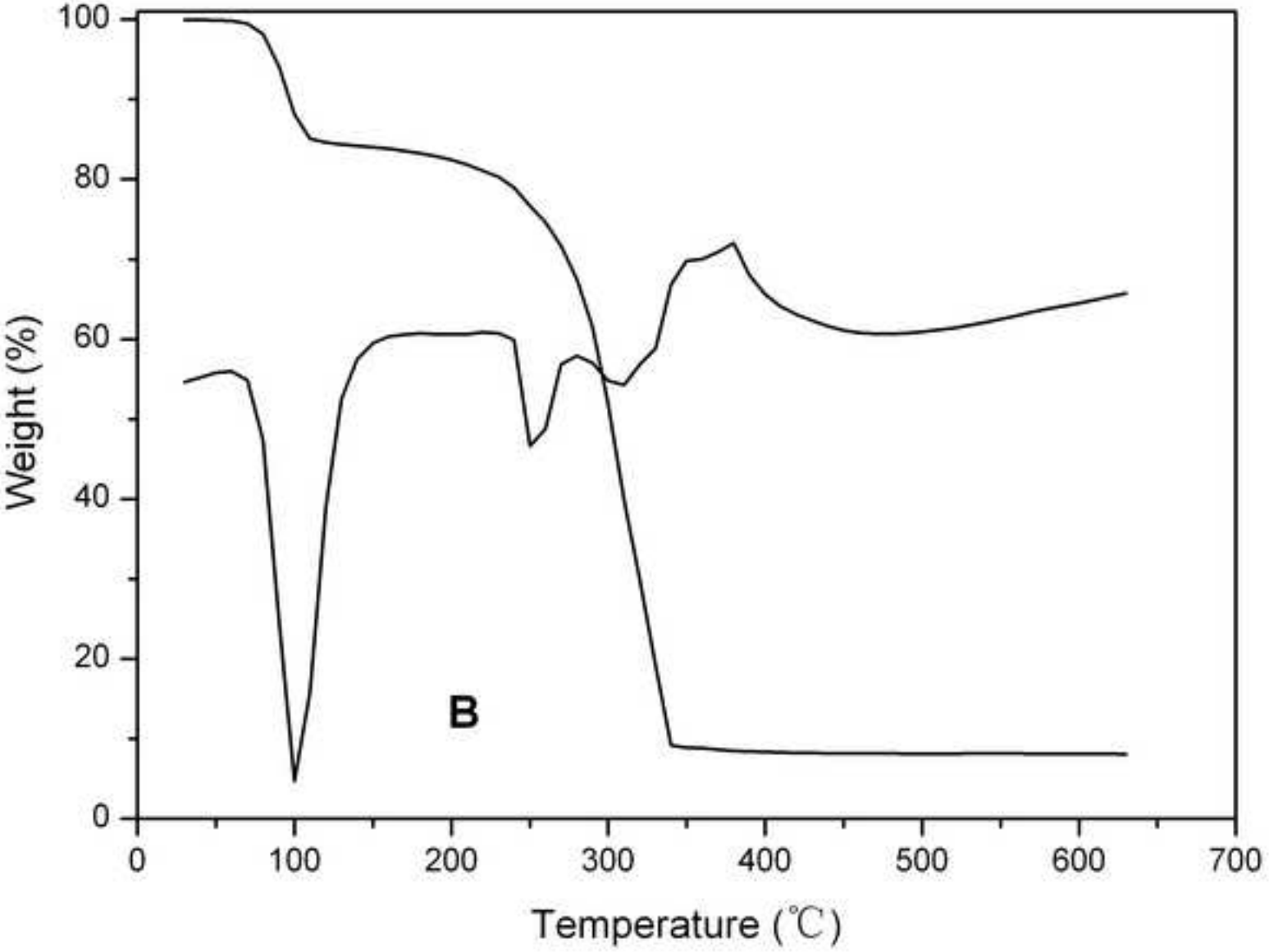
100
80
60
40
20
0
Weight (%)
B
0
100
200
300
400
500
600
700
Temperature (℃)

Figure2C

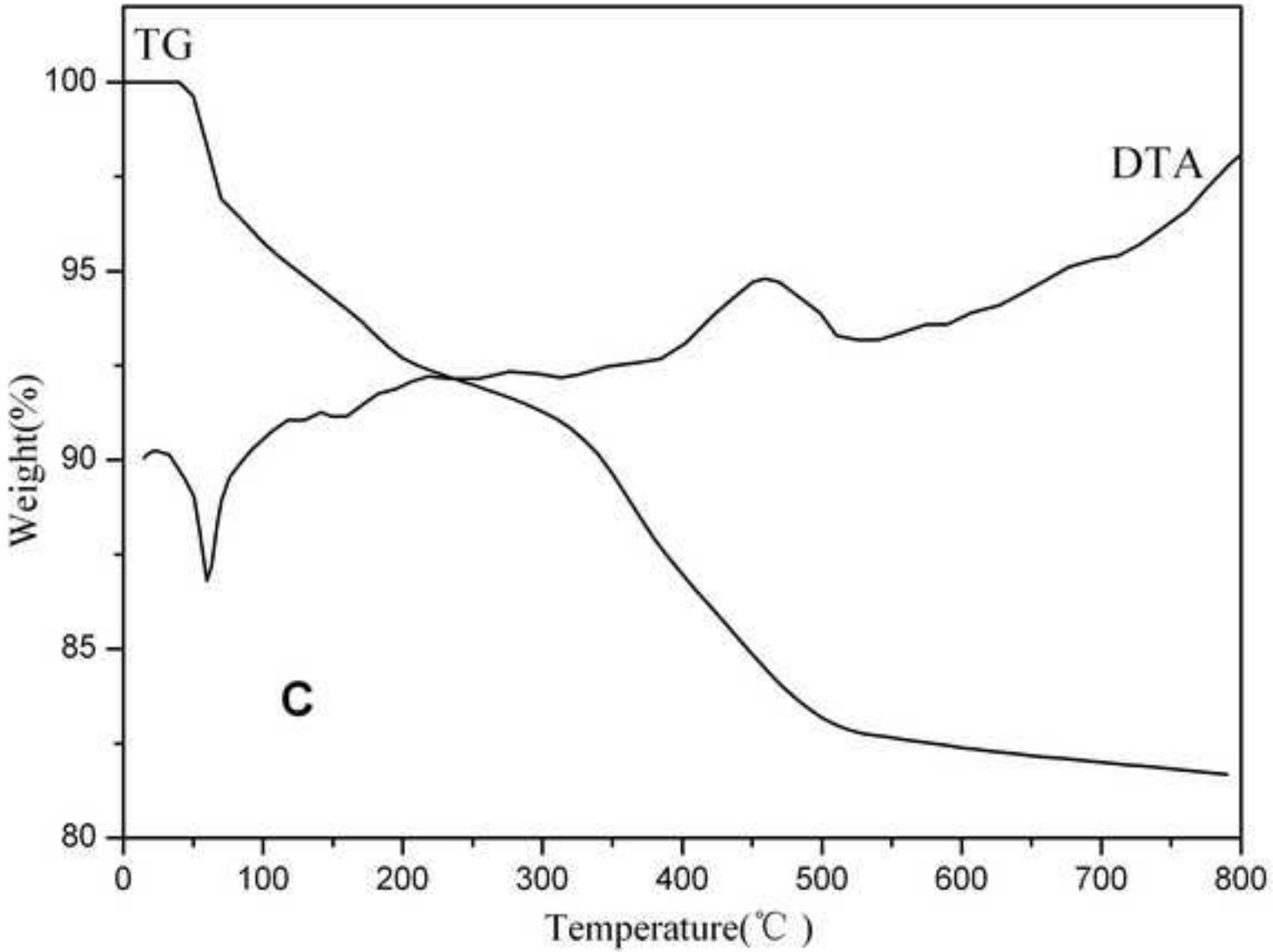
TG
DTA
100
95
90
85
80
Weight(%)
C
0
100
200
300
400
500
600
700
800
Temperature(℃)

Figure3

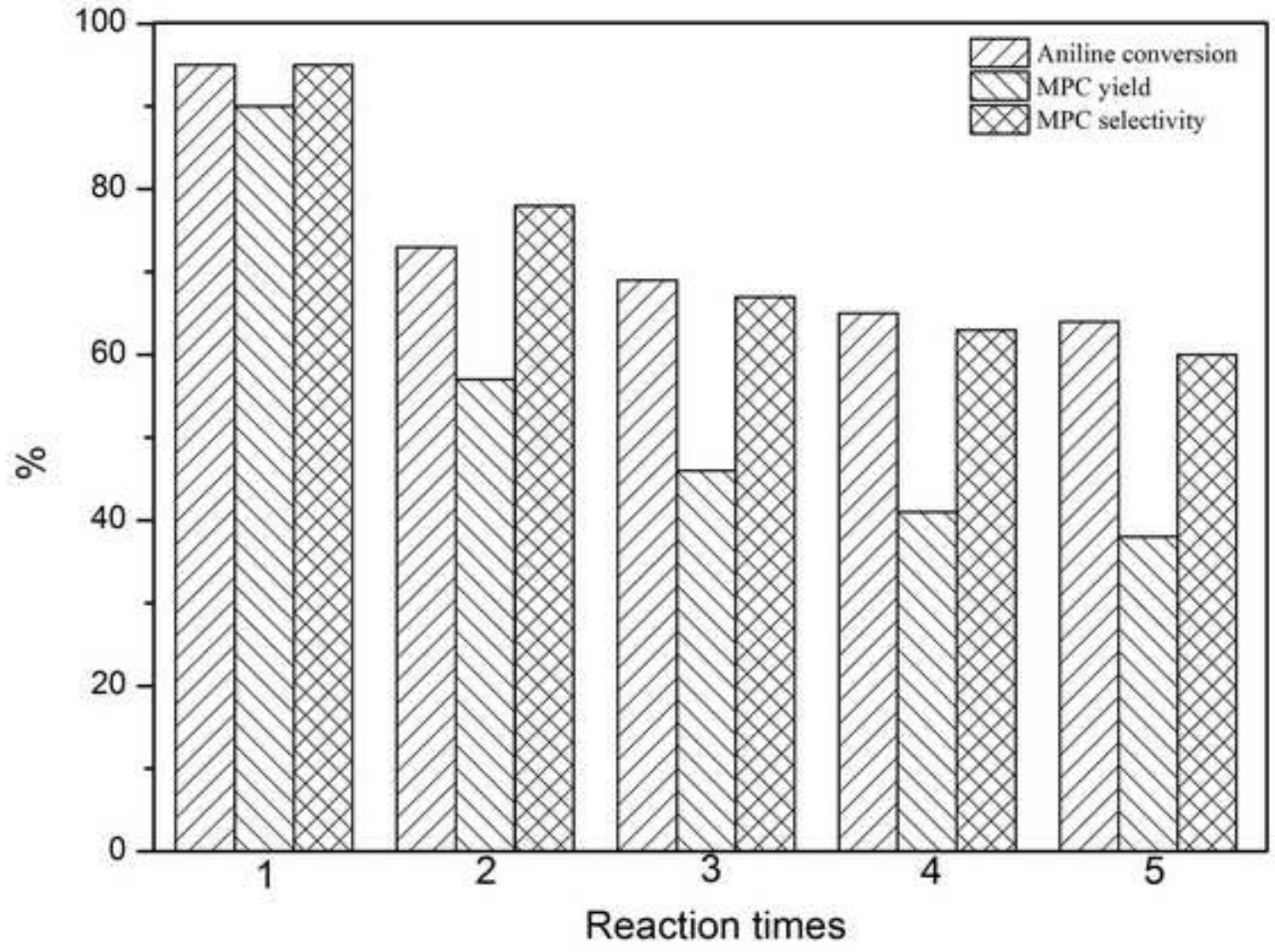
100
80
60
40
20
0
%
1
2
3
4
5
Reaction times
Aniline conversion
MPC yield
MPC selectivity

Figure4

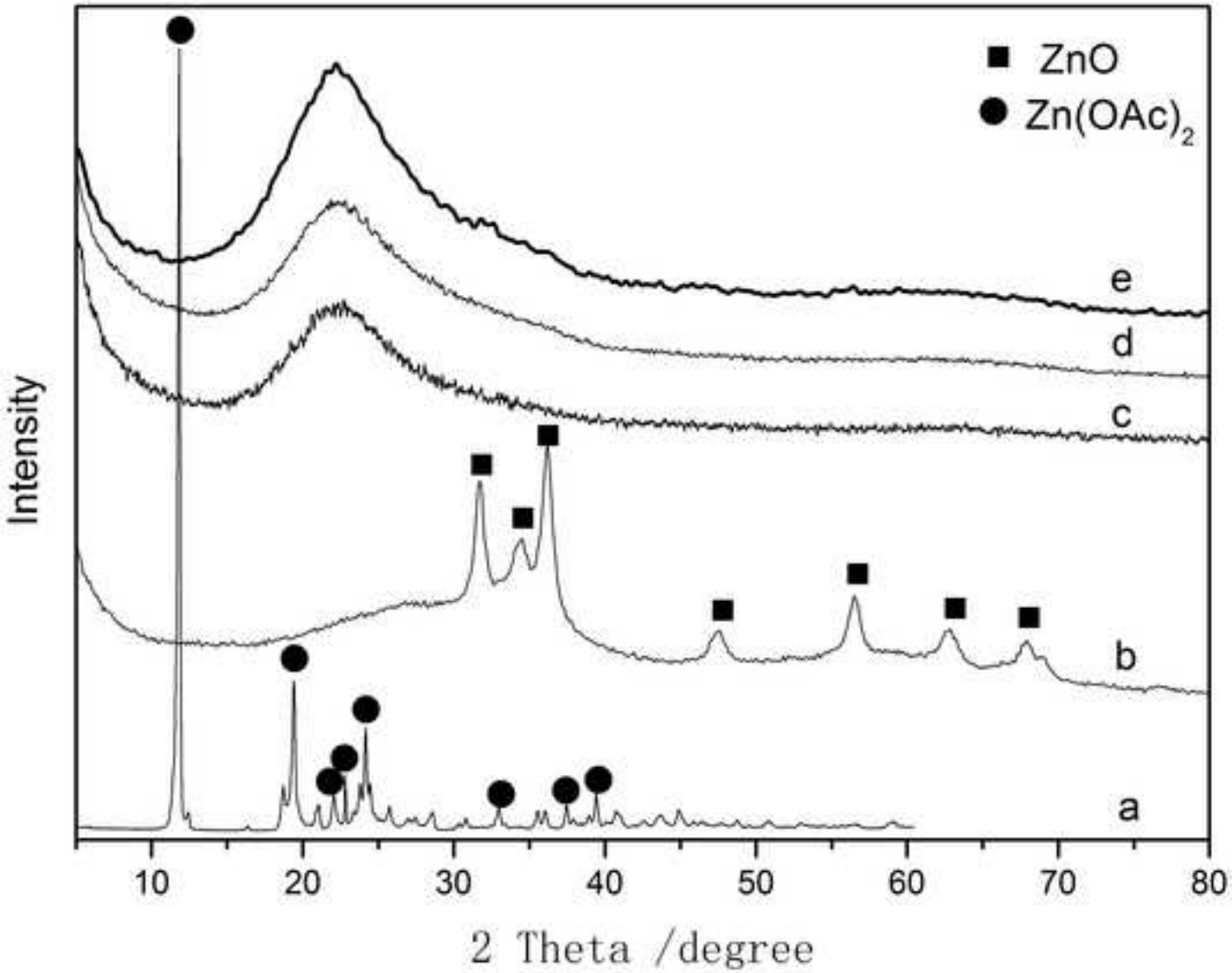
ZnO
Zn(OAc)2
e
d
c
b
a
Intensity
10
20
30
40
50
60
70
80
2 Theta /degree

Figure5

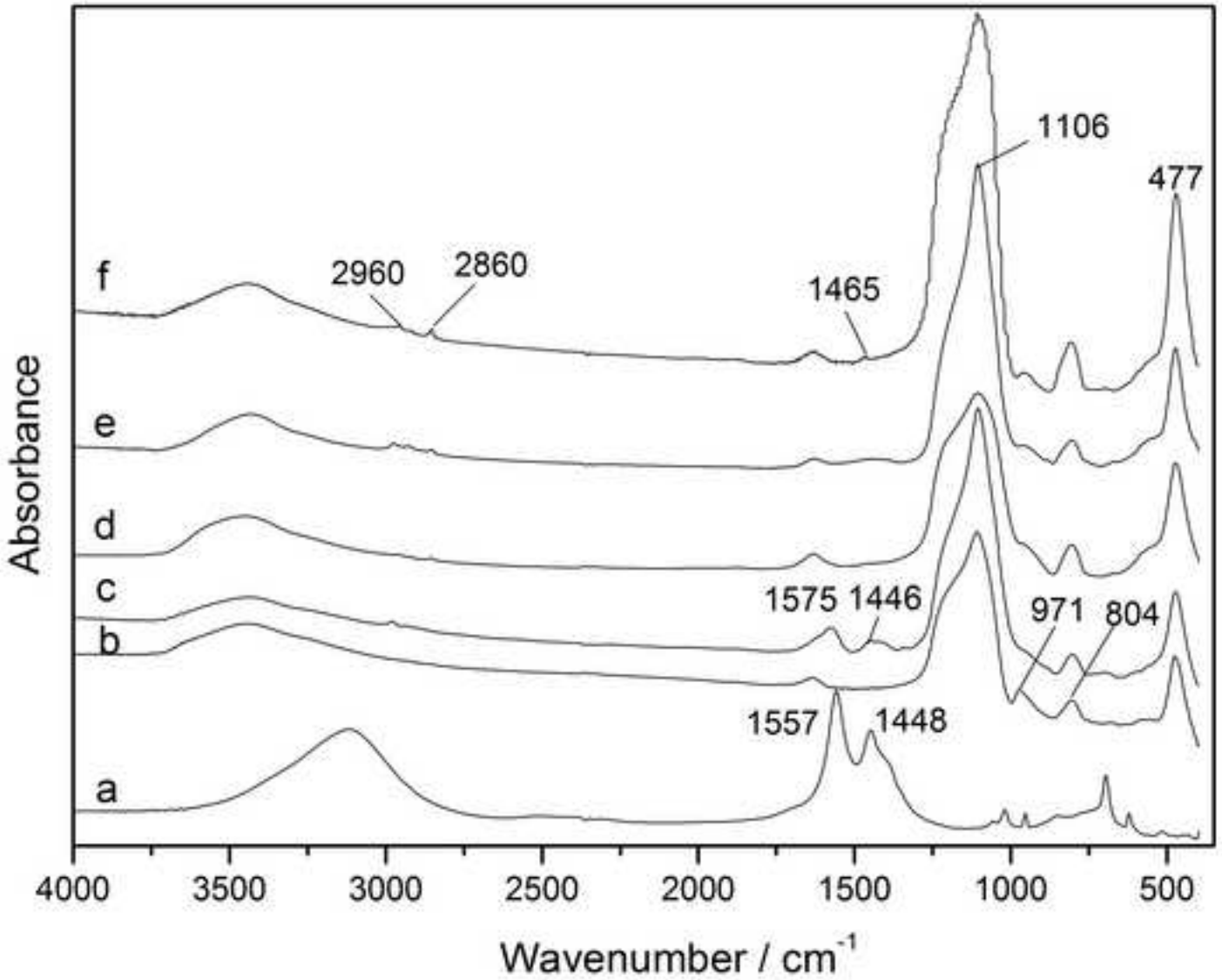
Absorbance
f
e
d
c
b
a
2960
2860
1465
1106
477
1575
1446
971
804
1557
1448
4000
3500
3000
2500
2000
1500
1000
500
Wavenumber / cm-1

scheme 1

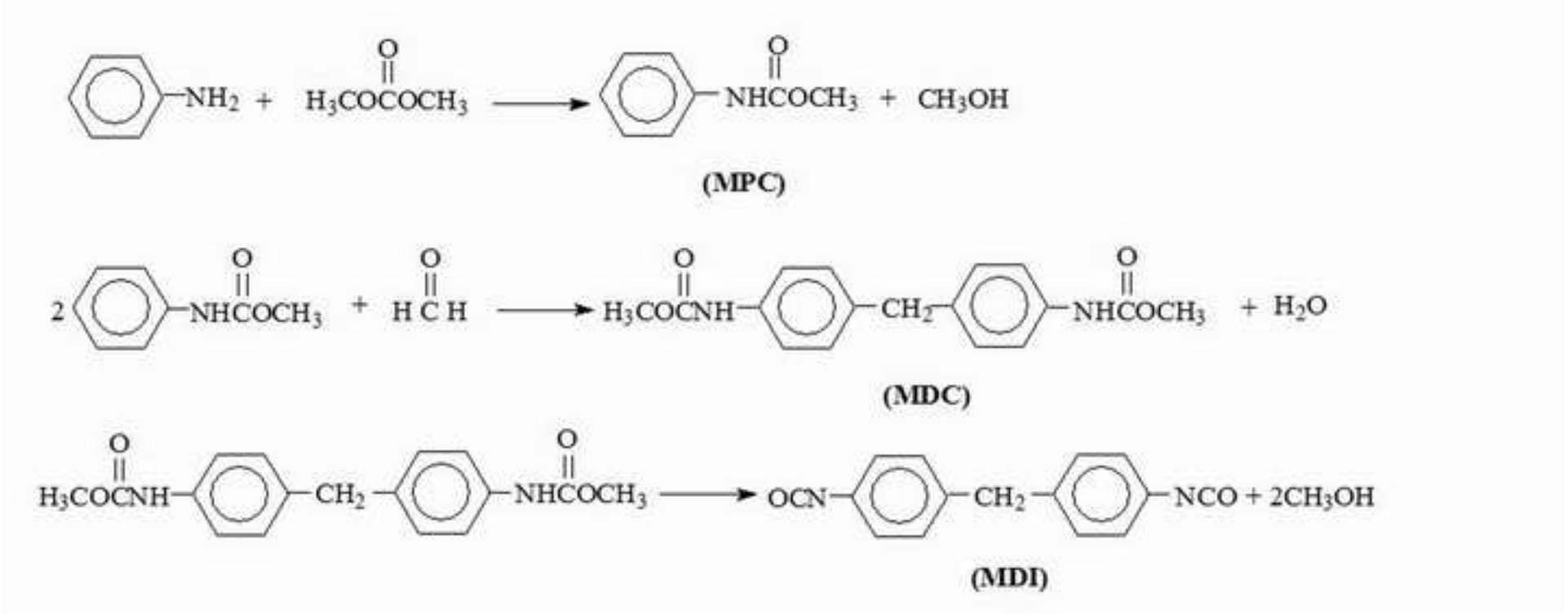
NH2 + H3COCOCH3
NHCOCH3 + CH3OH
(MPC)
2
NHCOCH3 + H C H
H3COCNH CH2 NHCOCH3 + H2O
(MDC)
H3COCNH CH2 NHCOCH3
OCN CH2 NCO + 2CH3OH
(MDI)

scheme 2

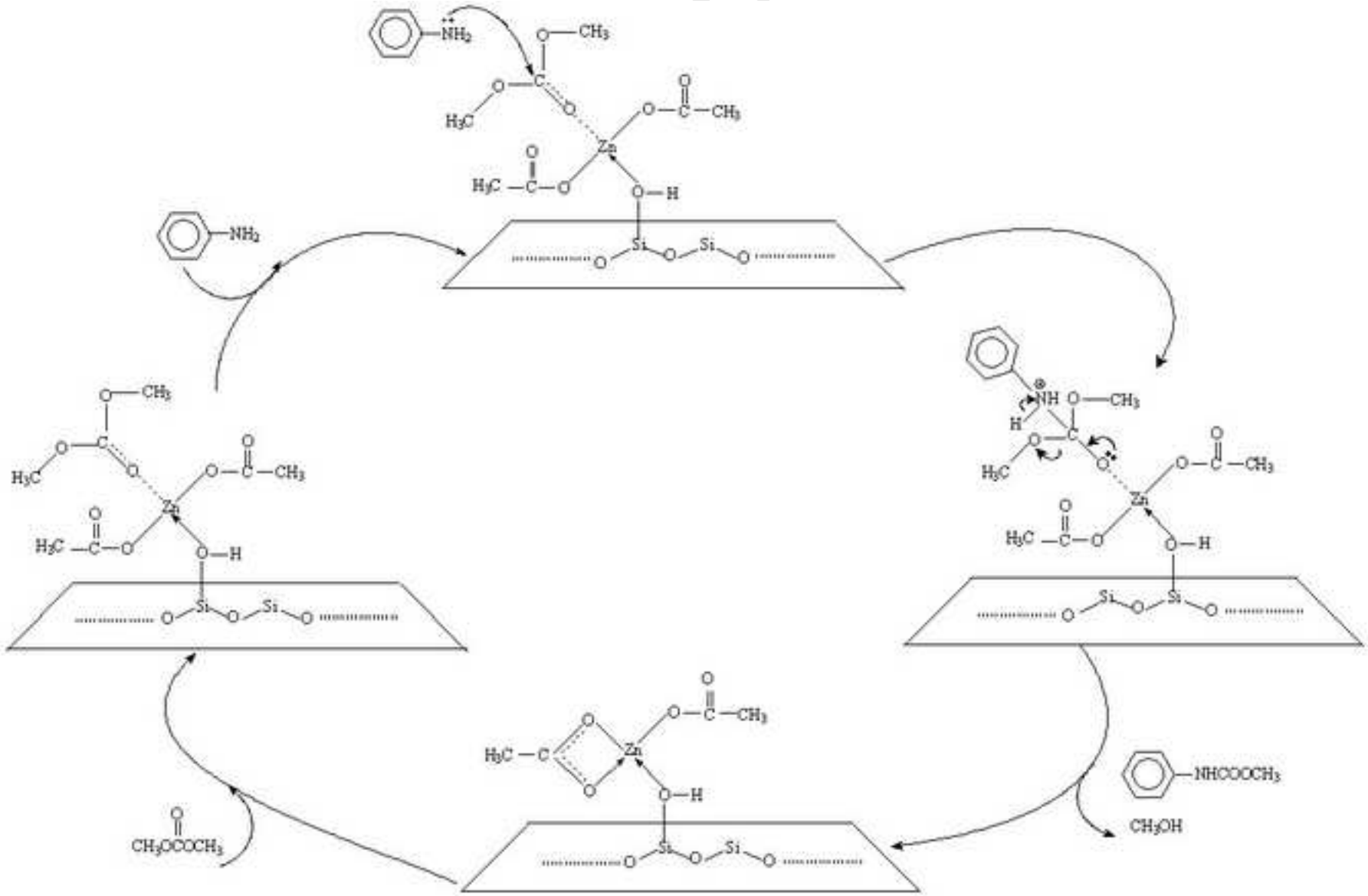
NH2
CH3
H3C
Zn
H3C —C—O
O—H
Si
O
O—C—CH3
NH
H
NHCOOCH3
CH3OH
CH3OCOCH3

Table 1 Effect of loading amount and calcination temperature on catalytic performance [a]

Entry[b]	$Zn(OAc)_2$ load (wt%)	Amount of Zn in catalyst (mol)	Calcination temperature (°C)	Aniline conversion (%)	MPC yield (%)	Product distribution (mol percent %)			
						NMA	MPC	DPU	DMA
1	2	3.1×10^{-5}	300	37.1	5.2	56.9	28.8	1.2	13.1
2	10	1.5×10^{-4}	300	95.4	87.7	7.2	90.6	0.2	2.0
3	20	3.1×10^{-4}	300	98.4	87.8	5.4	92.8	0.1	1.7
4	30	4.6×10^{-4}	300	98.1	93.8	4.9	93.5	0.1	1.5
5	35	5.4×10^{-4}	300	97.0	90.2	5.7	92.6	0.1	1.6
6	30	4.6×10^{-4}	400	98.0	89.5	6.1	90.7	0.1	3.1
7	30	4.6×10^{-4}	500	83.5	64.4	17.2	74.5	0.5	7.8
8	30	4.6×10^{-4}	600	36.6	13.3	49.9	35.4	0.7	14.0

[a] Reaction conditions: catalyst 0.28 g, DMC 0.2 mol, aniline 0.01 mol, 170 °C, 7 h.

[b] The catalyst was calcined for 2 h.

Table 2 Specific surface area, pore volume and pore size of the $Zn(OAc)_2/SiO_2$ catalysts

$Zn(OAc)_2$ load (wt%)	S_{BET} ($m^2 \cdot g^{-1}$)	Pore volume ($cm^3 \cdot g^{-1}$)	Pore size (nm)
0	297.5	1.8	25.0
2	289.9	1.7	23.6
10	254.8	1.6	23.5
20	223.6	1.4	21.9
30	193.5	1.3	21.2
35	189.6	1.3	18.5

Table 3 Catalytic activity comparison between $Zn(OAc)_2/SiO_2$ and $Zn(OAc)_2$

Catalysts	Amount of Zn in catalyst (mol)	Reaction time (h)	Aniline conversion (%)	MPC yield (%)	TON [c]
$Zn(OAc)_2$ [a]	4.6×10^{-4}	3	98.7	92.7	20.2
		5	98.8	96.5	21.0
		7	99.0	95.4	20.7
$Zn(OAc)_2/SiO_2$ [b]	4.6×10^{-4}	3	92.5	80.7	17.5
		5	97.9	89.8	19.5
		7	98.1	93.8	20.4

[a] Reaction conditions: Catalyst: 0.084 g, DMC: 0.2 mol, aniline: 0.01 mol, temperature: 170 °C.

[b] Reaction conditions: Catalyst ($Zn(OAc)_2$ loading: 30 wt%, calcination temperature: 300 °C): 0.28 g, DMC: 0.2 mol, aniline: 0.01 mol, temperature: 170 °C.

[c] TON = mol MPC/mol Zn

Table 4 Binding energy of Zn 2*p*3, Si 2*p* and O 1*s* in the different catalysts

Catalysts	Zn 2*p*3	Si 2*p*	O 1*s*
$Zn(OAc)_2$	1022.2eV	-	531.9eV
SiO_2	-	105.7 eV	534.7 eV
$Zn(OAc)_2/SiO_2$	1022.2eV	103.2eV	532.4eV